A NOVEL ROTATING TEMPERATURE AND RADIATION MAPPING SYSTEM IN SUPERFLUID He AND ITS SUCCESSFUL DIAGNOSTICS*

Q. S. Shu¹, T. Junquera², A. Caruette², O. Deppe ¹,M. Fouaidy² W.D. Moelter¹, M. Pekeler¹, D. Proch¹, D. Renken¹, C. Stolzenburg¹ ¹Deutsches Elektronen-Synchrotron (DESY), Notkestrasse g5, 22607 Hamburg, Germany ²Institute of Nuclear Physics (CNRS - IN2P3) 91406 ORSAY cedex, France

Abstract

A novel rotating temperature and radiation mapping system in He II has been developed to investigate field emission (FE) & thermal breakdown (TB) in TESLA 9-cell SRF cavities. More than 10,000 spots on a cavity surface can be analyzed in one turn with 5° stepping. 116 special surface scanning thermometers have been developed to measure surface temperature in He II. 32 photodiodes are employed to study the X-rays induced by FE. electrons. Each rotating arm holds 14 thermometers and 4 photodiudes. A unique driving and suspension system is designed to gently turn the 9 arms around the cavity and uniformly press the thermometers against cavity surfaces. A moving adapter device (pancakes) is designed for rotating a large number of electronic cables which become inflexible in superfluid He.

The T-R mapping system has successfully detected and diagnozed serious problems caused by FE and TB, and has played a significant role in cavity processing.

INTRODUCTION

Main Obstacles of High Gradient Cavities

Field emission (FE) and thermal breakdown (TB) are still the main obstacles preventing SRF cavities from confidently reaching Eacc = 25 MV/m (TESLA's goal) from existing operating levels of 5-10 MV/m^{1.2.3}. Most of the FE sources and TB defects on the inner RF surfaces of cavities were found to be submicro-sizes^{4.5} and activated only at high RF fields while cavities are in a superconducting state. It is impossible to directly observe the FE and TB on the inner surface of cavities during RF operation. Therefore, the main approach to understanding the FE and TB of cavities is to study the hot spots and X-rays (induced by impacting FE electrons) generated on the cavity surfaces during RF operation.

DESY's Rotating T-R Mapping System

Various temperature (T) mapping and X-ray (R) mapping systems have been developed at many laboratories around the world^{3,4,6,7,8}. The systems can be classified into two categories: (1) Fixed Mapping - thermometers or photodiodes are fixed on the surfaces of the cavity. (2) Rotating Mapping - thermometers or photodiodes are rotating against the surfaces of the cavity.

The Rotating T-R mapping system developed at DESY for TESLA 9-cell cavities combines measurements of T & R and employs special rotating scanning thermometers which were developed at INP Orsay.

Advantages.

- (1) Greatly reduce the number of sensors: The DESY T-R mapping analyzes 10,000 spots on the cavity surface using only 116 scanning thermometers. A stystem using fixed thermometers would require 10,000 thermometers to analyse the same spots on cavity.
- (2) Once an area is suspected, the sensors in DESY mapping system can be relocated to the suspect location during cryogenic-RF operation for additional analysis.
- (3) The mapping combinesT-R diagnotic systems to give information on both heating and x-rays for understanding the dynamic progress of cavity processing.

Challenges.

- (l) Fixed contacts and use of grease as bounding agent to enhance thermal contact between thermometer and surface being measured are essential to reach a high efficiency (particularly, in the case of He II). In a rotating system, neither fixed contact nor grease can be applied. A new type of thermometer was needed⁹.
 - (2) Due to TESLA cavity structure, thermometers can not reach the high risk areas of FE at cavity irises. A

^{*} Advances in Cryogenic Engineering, Vol. 41 Edited by P.Kittel, Plenum Press, New York, 1996

combined measurement of T & R was required.

- (3) The TESLA cavity has 9 cell (the largest cell number for low frequency cavities) with complex surface curves. The space in the cavity test cryostat is tightly constrained. Assuring satisfaction of 3-dimension tolerances at all moving contact points is a challenge.
 - (5) A fast data acquisition system was also needed to trace the dynamic progress.

We have overcome the above challenges and developed the rotating T-R mapping system. Since December 1994, the system has been successfully employed in diagnostic tests and played a significant role in cavity precessing 10.

TECHNOLOGIES DEVELOPMENT

Surface scanning Thermometer and Photodiode

The surface thermometer design as shown in Figure 1(A) is very close to the model developed earlier for the CERN's SRF cavity project by INP Orsay ^{10.11,12}. The sensitive part is an Allen-Bradley carbon resistor (100 Ohm, 1/8 W) housed in a silver block with a sensor tip of 1 mm diameter for the thermal contact to the external surface of the cavity. This housing is thermally insulated from the surrounding He II by an epoxy envelope (Stycast) moulded around the silver block and into a bronze piece which allows the sensor to be mounted in the rotating thermometric arm, The thermometer's tip must present a good contact with the cavity wall when scanning. Each thermometer has two independent manganin wires thermally anchored to the silver block with~15cm free length for connecting to each cell board (14 thermometers).

The complementary calibration test was performed by mounting the thermometers in the real operating conditions of the scanning device at different spring pressures and heat fluxes in He II and subcooled He (2.3K and one bar). The detailed results are presented in another paper⁹. In the case of He II, the efficiency is heater power dependant.

Commercial PIN silicon/S 1223-01 photodiodes are used as x-ray detectors in the mapping because of their small size (3mm \times ϕ 10 mm) and ultra-fast response. A simplified photodiode cross-section is shown in Figure 1 (B).

Rotating T-R Arms

As shown in Fig. 2, 14 thermometers and 4 photodiodes are mounted in each arm which is precisely machined to have the same curved surface as the cavity cell. Due to the reinforced structure of TESLA cavity, the thermometers can not directly touch the surfaces of the cavity iris. Considering that the electrical fields reach maximum at the iris, 4 photodiodes are located in the end of each arm to monitor FE induced X-rays while 14 thermometers are used to monitor the temperatures in the entire region between the irises of each cell¹³. Two springs located inside two holes in the body of the rotating arm are used to adjust the contact pressure. A printed circuit board is mounted on the side of the arm. All cables for the sensors are fed through a device, called moving adapter device or "pancakes", and then connected to a feedthrough on the top flange of the cryostat. Fig. 3 is the T-R mapping system.

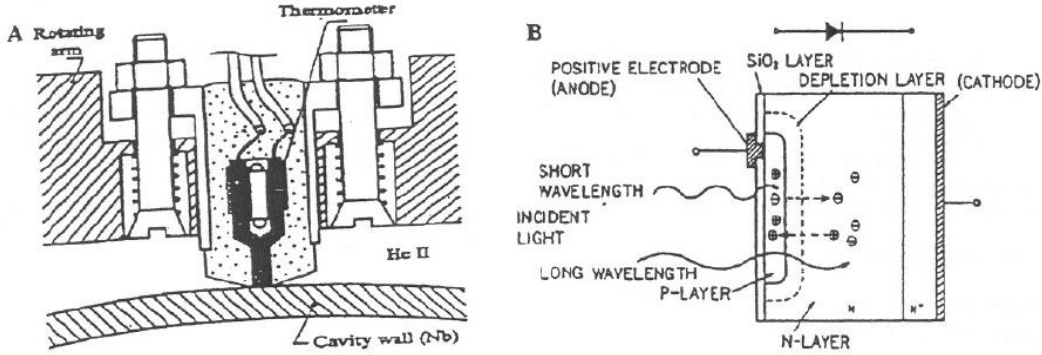


Figure 1(A) Cross section of a HeII surface scanning thermometer,(B) cross section of a photodiode

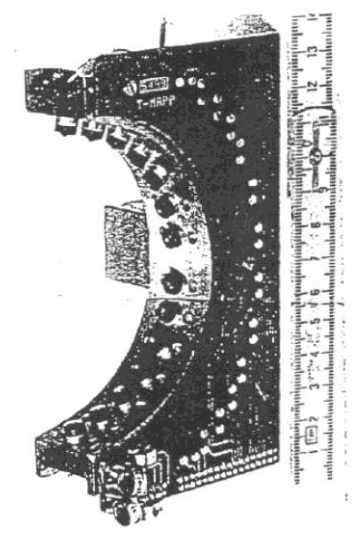


Figure 2. A picture of the rotating arm.



Figure 3. A picture of the T-R mapping system.

Driving and Suspension Frame (DSF)

A total of 116 surface scanning thermometers $(14\times7 + 9\times2)^{13}$ and 32 photodiodes are assembled into 9 rotating arms which are mounted in the DSF as shown in Figure 4 (A).

The most important consideration in the mechanical design is to assure the three dimension tolerance between the cavity surface and the tips of the 116 thermometers over the entire cavity surface (i.e. more than 10,000 points) are within ± 1 mm. The DSF has two centering rings to allow the axis of DSF as close to the axis of the cavity cells as possible. The rotating frame is suspended on two disks made of low friction materials. These structures enable the DSF in superfluid He to gently turn the arms around the cavity and uniformly press the thermometers (through the spring-holder structure, force=100 g per thermometer) against the cavity surfaces. Driven by a computer-controlled stepping motor, the T-R arms can be automatically turned to any position on the cavity surface with a accuracy of ± 1 degree.

Moving Adapter Device (MAD)

A large number of electronic measuring cables have to move with the rotating arms when the T-R mapping rotates. These cables become very rigid in LHe. A moving adapter device¹³ wag successfully designed to overcome the problem as shown in Figure 4 (B). Each pancake has two rings. The inner ring is mounted in the moving DSF and tums with the DSF around the cavity. Its outer ring is fixed with cavity supports. One end of each 64-wire-cable is connected to the inner moving ring and the cables make 9 turns around the inner ring of the MAD while the other end of the cables connects to the outer fixed ring, When the DSF turns 360° around the cavity, the cables only make relatively short movement inside the MAD. The space in the TTF vertical cryostat is very constrained which makes the MAD design even more difficult. The MAD has been tested and functions well in many cavity experiments.

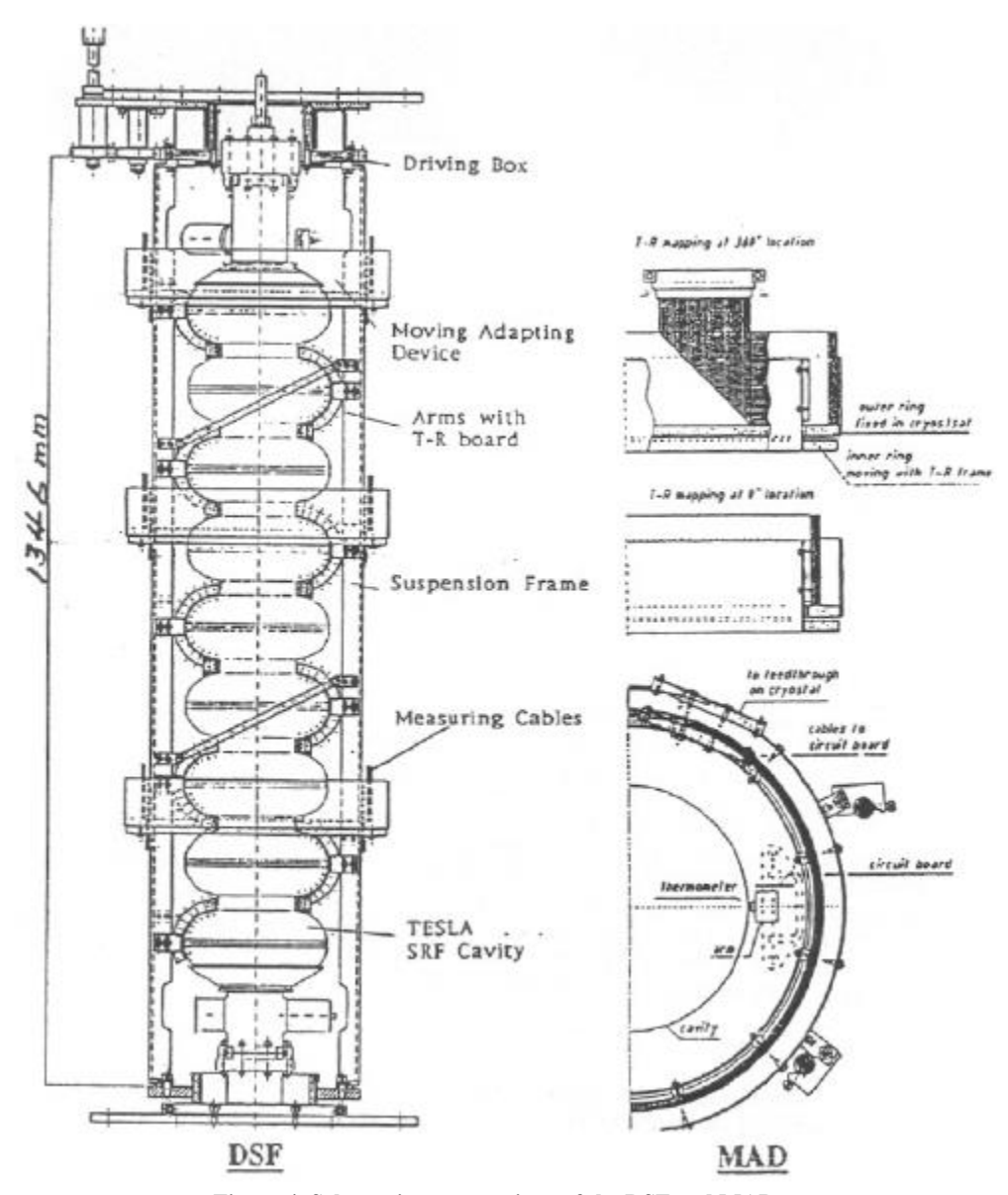


Figure 4. Schematic cross sections of the DSF and MAD.

Fast Data Acquisition and Test Procedure

Two Ge-thermometers and three additional scanning thermometers are used to monitor the change of bath temperature during measurement. To check the photodiodes two small lights are placed in the DSF. Maps can be taken with auto-scanning of entire cavity surface or scanning with time in a fixed position. The temperature change $\triangle T$ is made by comparison of measurements of RF power on and off (also, the bath temperature changes are subtracted from the total $\triangle T$). The effective resolution of temperature measurement is less than 5 mK. One longitudinal measurement in a fixed angular position can be completed in less than 10 ms. All data taken, control and display are performed through a multiplexer by a Sun-station computer with a LabView language program 14.

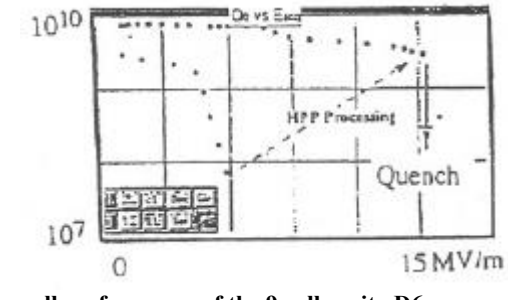
RESULTS, ANALYSIS & DIAGNOSTIGS

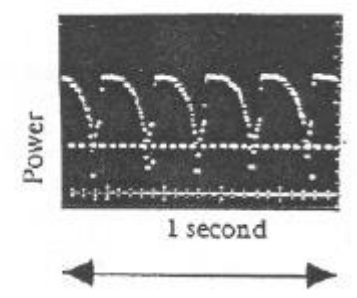
The T-R mapping has been successfully employed in the diagnostic testing of TESLA SRF cavities. We will briefly introduce some of the more interesting results here, A detailed test report will be presented in the "1995 SPF Superconducting Workshop".

Detection of Thermal Breakdown

We use the TESLA 9-cell cavity (D-6) as an example shown in Figure 5. This cavity has been heat treated with Ti-purification at 1400° C for 4 hrs and a test sample has a RRR of about 500. At first, the cavity was limited by severe FE at Eacc = 4 MV/m and Q dropped to 8 x 10^{7} , Fig. 5 (A). With RF power processing, the FE events were eliminated and the T-maps show the heating areas by FE gradually disappeared. Finally the cavity reached Eacc= 12.5 MV/m through a high RF pulse peak power processing (HPP) and then limited only by a quench.

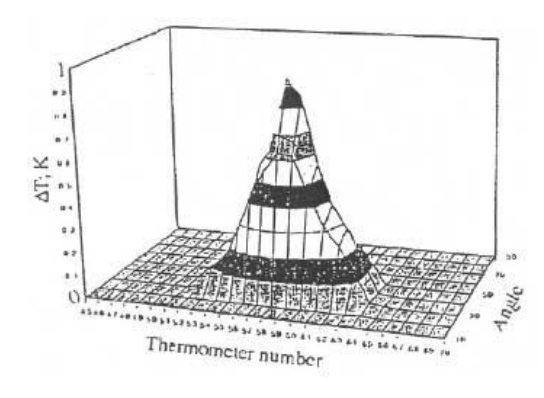
While scanning the entire surfaces of the 9-cell cavity, the T-mapping located a strong heating area centred at the equator of the cell-5 over l0 thermometers between the 10° to 50° longitude as shown in Fig. 5 (C). To further study the TB event, we relocated the T-R arm to the heating area, moved it by 5° angular steps and found the hottest spot to be near 35°. Finally we moved the arms to 35°, turned on the RF power in CW mode and observed continuing quenches and recoveries of the cavity as shown in Fig 5 (B). Simultaneously, we continuously took temperature measurements at this fixed location. Fig. 5 (D) shows a dynamic progress of the temperature changes at 35° as a function of time. The highest temperature measured on the outer surface of the cavity is above 5 K and the quench was limited to one cell and did not propagate to adjacent cells.

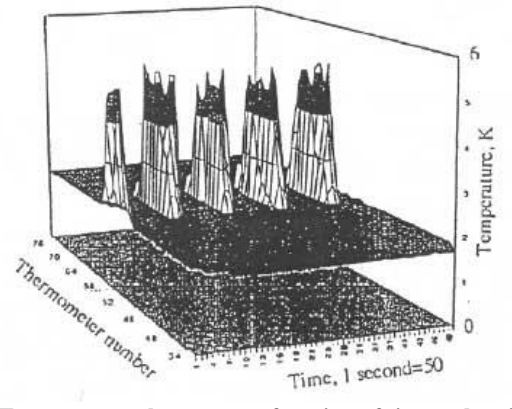




(A) Overall performance of the 9-cell cavity D6.

(B) Oscilloscope traces of transmitted power during continuing TB (quench) of the cavity.





(C) The detected heating area due to TB (quench)at the equator of the cell-5. recovery.

(D) Temperature changes as a function of time at longitudinal of 35° of the cell-5 during continuing quench &

Figure 5. The dynamic progress of a cavity thermal breakdown (quench) detected by the T-R Mapping.

These results indicate that HPP is very effective in eliminating FE^{15} , but not for TB. The tests tell us that there may be a combination of local defects at cell-5 and existence of a low thermal conducting thin layer (due to Ti-purification) on the cavity. Optical observation after test showed a deep scratch on the inner surface near the equator and close to 35° of cell-5. We are planing to take an additional 50 μ m of material from the inner surface and test it again.

Identification or FE Heating and Emitter Location

In investigating FE, we first use T-R mapping to identify the landing areas of FE electrons and then find out the locations of emitters with simulations of FE electron trajectories. we use a TESLA prototype 9-cell cavity (-1) as an example. It has reached 20 MV/m as shown in Figure 6 (A). Prevjously, cavity(1) had been limited by thermal breakdown at about Eacc = 10 MV/m. Afterwards, the cavity -1 was heat treated at 1400° C with Tipurification. We then removed $80 \mu \text{m}$ of material from the inner RF surface and $30 \mu \text{m}$ from outer side by

chemistry, followed by high pressure rinsing.

Locating of Heated Areas and Intensity

In the test, cavity -1 was initially stopped by heavy field emission at point A (figure 6) at 11.2 MV/m with a Q of 8.5×10^8 . The T-map, figure 6 (B) indicates an important heated region delimited by 12 thermometers (#53 to #64) centred close to the equator of the 5th cell, between the 110° to 200° angles. Outside of this region the heating is very low. The $\triangle T$ value in this region is 100mk - 3.3K. The y-axis of Figure 6(B) is the thermometer number from 0, close to the top iris of cell-1, to 116, close to the bottom iris cell-9. The x-axial represents the angular location on the cavity surface.

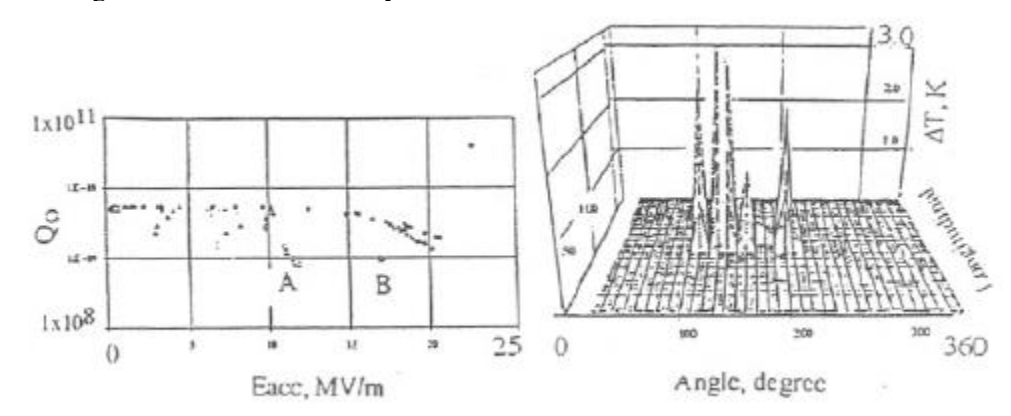


Figure 6. (A) Overall RF performance of the TESLA cavity -1.

(B) FE heating area responsible for the Q dropping and limit of Eacc.

Analysis of Thermal Performance

The experimental data obtained with the T-R mapping is consistent with the thermal analysis if we make the following assumptions: high efficiency of thermometer at high heat flux, heat transfer governed by Kapitza regime, and electron trajectories impacts over a large area. The magnetic field heating at equators of the 5th cell, for Eacc=11.2 MV/m and Rs=30 n Ω , gives only \triangle T=5 mK. The power related to the electron FE, Pelec=173 W, is focusing on local region.

The very high value $\triangle T$ measured in this region (100mK-3.3K) can only be explained by assuming that the efficiency of a scanning thermometer increases strongly with the heat flux density at the interface between the cavity wall and HeII. Such a high heat flux density is slightly less than the critical heat flux densities reported in experiments with metallic flat heaters in HeII¹⁶. So it is believed that the heat transfer is in the regime governed by Kapitza conductance. The integration of the product of Kapitza conductance and $\triangle T$ over the heated region leads to a total heat power going to He bath: $Q\sim100$ W. This value is consistent with the RF measurements of the experiment.

Identifying of FE Emitter Location

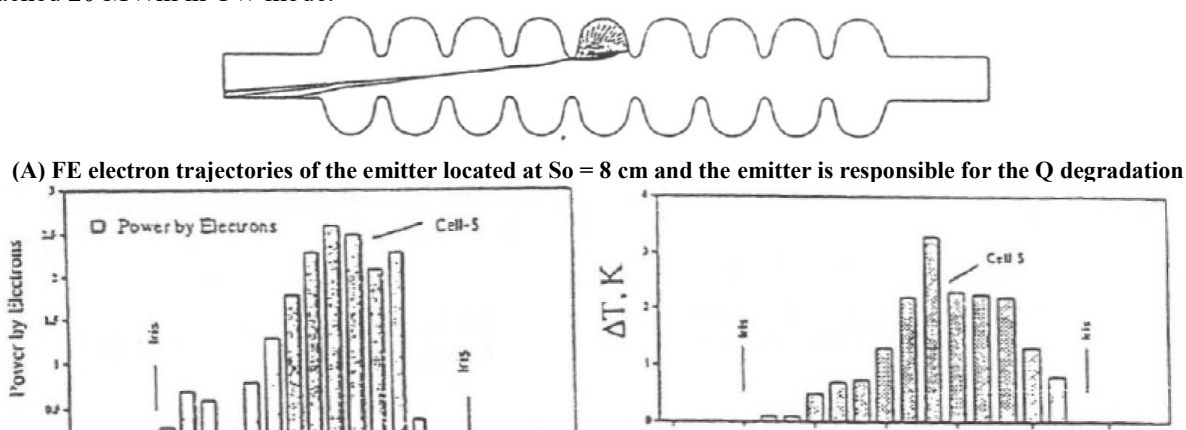
Locating origins of FE and TB is very important to understand the influence of various cavity processing and also to a guided reparation of defected cavities. However, the measured hot spots only indicate the landing of impacting FE electrons, but not the emitter.

The simulation of FE electron trajectories demonstrate the following interesting results: FE electrons from an emitter can impact over a very large area, the shape of trajectories are sensitive to emitter location (So), and emitters responsible for the heating areas (shown in figure 6 B) can be successfully identified. Since electron trajectories, impacting electron energy and power deposition distribution (dP/ds vs. s) are controlled by the Eacc and So. A series of simulations are performed by changing So at Eacc=11.2 MV/m, assuming emission enhancement $\beta = 200$, Se (emitter area) = $1 \times 10^{-13} \text{m}^2$. It is found that an emitter located at So=8 cm (at the iris area) has electron trajectories shown in figure 7 (A). Its power distribution (dP/ds vs. s) in Figure 7 (B) seems to be very close to the shape of the measured temperature distribution, Figure 7 (C). It indicates that heated areas at the equator (usually by defects) can also be caused by FE. The β and Se of the candidate emitter were adjusted to fit with the thermal analysis and RF experimental data. For instance, at Eacc=11.2

MV/m, if Se= 1×10^{-13} m², $\beta = 400$, the total mean power landed over RF period is 10W.

Finally, the high pulse RF power processing (HPP) was introduced to the cavity (150KW) and successfully

eliminated the field emitters. Another T-map also witnessed the FE elimination. After HPP, the cavity finally reached 20 MV/m in CW mode.



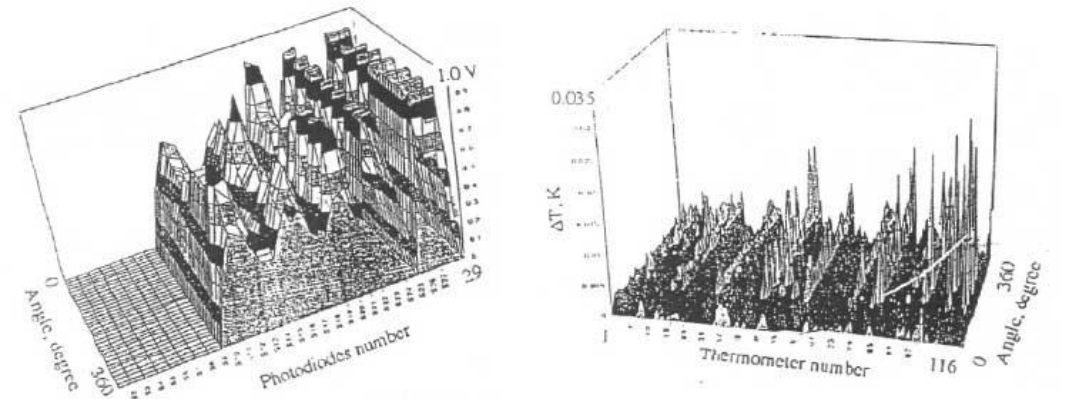
(B) Power distribution contributed plot from

Location Along Carity

(C) Experimental longitudinal ΔT

Thermometer Number

by impacting FE electrons from So=8cm. T-map data of Figure 6 B fixed at 1-10° Figure 7. A comparison of computer simulation of the FE emitter with the experimentally heated areas.



(A) An X-ray map in which the strong radiation closed to the cavity irises.

(B)A T-map taken in the same time as Fig 8 (A) shows that the FE heated areas are also located mainly in cavity irises.

 $\label{thm:comparison} Figure~8.~A~comparison~of~the~X-ray~map~with~the~T-map~in~the~same~9-cell~cavity~Information~from~X-Ray~Maps$

A large number of radiation maps of X-rays induced by FE electrons were also observed. In general, information from X-ray maps are in consistent with that obtained from T-maps. As we mainly discuss the technical areas relevant to low temperature science here, the X-ray maps and analysis will be presented at the 1995 SRF superconducting workshop (Saclay, France). Figure 8 (A) shows an X-ray map recorded during a cavity processing, while figure 8 (B) presents the T-map taken on the same cavity and in the same time.

CONCLUSION

The T-R mapping system for TESLA 9-cell cavities was commissioned and successfully analysed and diagnosed the problems with the TESLA cavities caused by FE and TB. The information learned from T-R mapping results has played a significant roles in cavity processing and will be very valuable in further guided reparation of some cavities.

ACKNOWLEDGEMENT

We sincerely thank P. Kneisel (CEBAF), W. Weingarten (CERN), H. Padamsee, M. Champion (Fermilab), C. Pagani (INFN). B. Bonin (Saclay) and G. Wueller, R. Roeth (Wuppertal) for many fresh discussions and hints. Sincere thanks are also presented to our DESY colleagues in the cryogenic group, vacuum group, mechanical group, MHF group for their support.

REFERENCES

- [1] D. Proch (editor, Procceedings of the 5th workshop on RFS, Hamburg, Aug., 1991. (status report, p5, p23, p37, p44, p84, ans p245) published by DESY.
 - R. Sundelin (editor), Proceeedings of the 6th workshop on RFS, Newport News, Oct.,1993 (status report, p33, p49. p67. p77, p131, p173) published by CEBAF.
- [2] H. Padernsee, Applied Supercond. Conf., Boston, 1994.
- [3] Q.S. Shu et al., IEEE transaction, Vol. 27, No. 2, 1991
- [4] B. Bonin et al., Proceedings of the 6th workshop on RFS, 1993.
- [5] R. Roth and G. Muller et al., Proceedings of the 5th (and 6th) workshop on RFS, DESY 1991 (and CEBAF, 1993).
- [6] Ph. Bernard et al. Nucl. Inst & Methods in Phys. vol 190.
 Ph. Bernard et al. & S. Buhler et. al, the 5th (and 6th) workshop on RFS, DESY 1991 (and CEBAF, 1993).
- [7] Q.S. Shu et al., Nucl Inst & Methods in Phys A278. 1989.J.Knobloch et al., SRF 94-0419-03, Cornell Univ., 1994
- [8] M. Fouaidy et al Proc 5th workshop on RFS, DESY,1991.
- [9] T. Junquera et al. TTP 14, Dallas, TX. PAC/95, May 1995.
- [10] Q.S. Shu et al., TTP19, Dallas TX. PAC/95, May 1995.
- [11] R. Romijn, W. Weingarten, IEEE Trans. on Magnetics, Mag. p. 1318, 19(1983).
- [12] S. Buehler et al., proceedings of the 6th workshop on RFS, Newport News, published By CEBAF, Oct. 1993.
- [13] Q.S. Shu et al. TESLA Weekly Meeting, February, 1995, DESY, Hamburg.
- [14] M. Pekeler, internal tech. note to be in Ph. D. thesis, 1995.
- [15] J. Graber et al., Nucl. Inst & Methods in Phy. A278. 1989.
- [16] A. Kashani, S. W. Van Sciver, Cryogenics 25, 1985.